Science of the Total Environment 642 (2018) 1–11

Contents lists available at ScienceDirect

Science of the Total Environment

journal homepage: www.elsevier.com/locate/scitotenv

Effects of water stress on water use efficiency of irrigated and rainfed wheat in the Loess Plateau, China

Ning Jin [a], Wei Ren [b], Bo Tao [b], Liang He [c], Qingfu Ren [a], Shiqing Li [a], Qiang Yu [a,d,e,*]

[a] State Key Laboratory of Soil Erosion and Dryland Farming on the Loess Plateau, Northwest A&F University, Yangling 712100, China
[b] Department of Plant and Soil Sciences, College of Agriculture, Food and Environment, University of Kentucky, KY 40506, USA
[c] National Meteorological Center, Beijing 100081, China
[d] College of Resources and Environment, University of Chinese Academy of Science, Beijing 100049, China
[e] School of Life Sciences, University of Technology Sydney, P.O. Box 123, Broadway, NSW 2007, Australia

HIGHLIGHTS

- The ratio of irrigated to rainfed winter wheat in the Loess Plateau was examined.
- Maximum light use efficiency and harvest index of winter wheat were estimated.
- Higher yield and actual evapotranspiration were found in irrigated winter wheat.
- Water use efficiency decreased more rapidly in rainfed wheat under water stress.

GRAPHICAL ABSTRACT

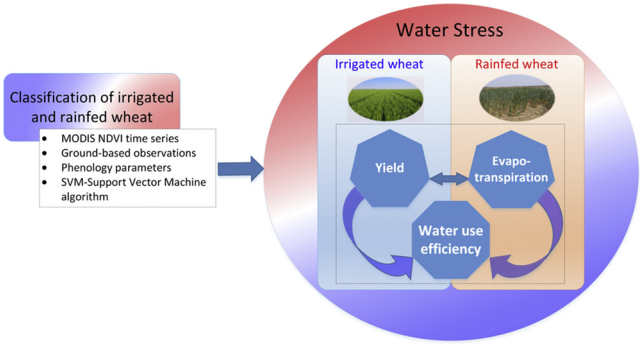

ARTICLE INFO

Article history:
Received 9 January 2018
Received in revised form 1 June 2018
Accepted 3 June 2018
Available online 14 June 2018

Editor: D. Barcelo

Keywords:
Water use efficiency (WUE)
Irrigated and rainfed wheat
MODIS NDVI time series
Water stress
Light use efficiency model

ABSTRACT

The Loess Plateau, the largest arid and semi-arid zone in China, has been confronted with more severe water resource pressure and a growing demand for food production under global changes. For developing sustainable agriculture in this region, it is critical to learn spatiotemporal variations in water use efficiency (WUE) of main crops (e.g. winter wheat in this region) under various water management practices. In this study, we classified irrigated and rainfed wheat areas based on MODIS data, and calculated the winter wheat yield by using an improved light use efficiency model. The actual evapotranspiration (ETa) of winter wheat and the evapotranspiration drought index (EDI) were also investigated. Then we mainly examined the synergistic relationship between crop yield, ETa, and WUE, and analyzed the variations in WUE of irrigated and rainfed wheat under water stress during the 2010–2011 growing season. The results suggested that winter wheat in the Loess Plateau was primarily dominated by rainfed wheat. The average yield of irrigated wheat was 3928.4 kg/ha, 22.2% more than that of rainfed wheat. High spatial heterogeneities of harvest index (HI) and maximum light use efficiency (ε_{max}) were found in the Loess Plateau. The ETa of irrigated wheat was 10.2% more than that of rainfed wheat. The ratio of irrigated and rainfed wheat under no water stress was 31.55% and 17.16%, respectively. With increasing water stress, the WUE of rainfed wheat decreased more quickly than that of irrigated wheat. The WUE variations in winter wheat under water stress depended strongly on the synergistic effects of two WUE components (crop yield and ETa) and their response to environmental conditions as well as water management practices (irrigated or rainfed). Our findings enhance our current understanding of the variations in WUE as affected by water stress under various water use conditions in arid and semi-arid areas.

* Corresponding author at: State Key Laboratory of Soil Erosion and Dryland Farming on the Loess Plateau, Northwest A&F University, Yangling 712100, China.
E-mail address: qiang.yu@uts.edu.au (Q. Yu).

https://doi.org/10.1016/j.scitotenv.2018.06.028
0048-9697/

1. Introduction

The growing water demand due to rapid socio-economic development is not compatible with the limited water resources, and the imbalance between water supply and demand for industry, agriculture, and domestic water is becoming more severe (FAO, 2010). In Northwestern China, irrigation water accounts for over 90% of the total water use (Shen et al., 2013). The over-exploitation of ground water and low water use efficiency (WUE) are also major problems in agricultural water use (Zhang et al., 2004; Mo et al., 2005), which may compromise the capacity to cope with the growing food demand and the shortage of water resources in the future (Molden et al., 2003; Bastiaanssen and Steduto, 2017). WUE reflects the relationship between photosynthetic production of vegetation and water consumption (Mo et al., 2005; Usman et al., 2014; Xie et al., 2016). An additional 5600 km^3 of water is estimated to be lost to the atmosphere through evapotranspiration (ET) by 2050 if the crop WUE does not improve (Falkenmark and Rockström, 2004). Improving the WUE can be achieved by increasing the production per unit of water consumed, or reducing the amount of water consumed per unit yield of production.

The Loess Plateau is one of the most fragile and ecologically sensitive regions in China. During the winter wheat growing season, the water deficit is severe and precipitation generally cannot meet the water requirements for crop growth and development. Irrigation is thus needed to ensure crop yield. Over recent decades, the Loess Plateau has seen obvious increases in drought frequency, duration, and severity (Jiang et al., 2016). Plants tend to maintain a high WUE under water limited conditions to enhance their ability to absorb water and reduce the effects of water deficit (Reichstein et al., 2007; Tian et al., 2011). However, some studies suggest that, under severe water stress, the WUE may reduce significantly with increasing water stress (Reichstein et al., 2002; Dong et al., 2011). The variability of WUE under water stress is associated with considerable uncertainties due to the lack of information regarding regional water management practices (irrigated versus rainfed) and climatic factors in the Loess Plateau (Lu et al., 2016; Zhang et al., 2016; Wang et al., 2018). Therefore, it is important to analyze the influence of drought on WUE and to improve our understanding of WUE as a function of water stress in the Loess Plateau.

Generally, water management strategies differ for irrigated and rainfed wheat (Zwart and Leclert, 2010). For irrigated wheat, they are to improve the WUE and increase crop yield, whereas for rainfed wheat, they are to make full use of natural precipitation to achieve a stable crop yield. The actual evapotranspiration (ETa), yield, and WUE are significantly affected by water management practices. The yield of irrigated wheat can be 2.3 times higher than that of rainfed wheat during drought years in the Loess Plateau (Jin et al., 2016). In recent years, the WUE for irrigated and rainfed crops has been widely studied at a range of spatial scales (Mo et al., 2005; Liu et al., 2007; Suyker and Verma, 2010; Tian et al., 2011; Tang et al., 2014). However, differences in water availability in the Loess Plateau were less considered for estimating WUE from remote sensing data or from crop models (Bu et al., 2015; Zhang et al., 2016, 2017). This may reduce the reliability of the estimated WUE.

The development of remote sensing technology now allows us to monitor the surface-energy distribution, vegetation growth, and water conditions. This offers an opportunity to evaluate the interaction between carbon and water cycles in the context of climate change at large spatio-temporal scales. The remote-sensing-based light use efficiency (LUE) model has been widely used to estimate the net primary production (NPP), crop growth, and yield formation (Lobell et al., 2003; Gitelson and Gamon, 2015). The harvest index (HI) and maximum LUE (ε_{max}) are two important parameters in LUE models. These two parameters are generally treated as empirical constants, which cannot reflect their spatial heterogeneities and may induce uncertainties into the estimated crop yield (Lobell et al., 2003; Tao et al., 2005; Zhang et al., 2016).

The scientific objectives of this study are as follows: (1) to use the support vector machine (SVM) algorithm based on the phenological parameters extracted from MODIS normalized difference vegetation index (NDVI) to account for the different water availabilities for winter wheat in the Loess Plateau and classify irrigated and rainfed wheat in the Loess Plateau; (2) to improve the estimated wheat yield by considering the spatial variabilities of ε_{max} and HI; and (3) to evaluate the synergy between ETa, yield, and WUE, and the variation of WUE as a function of water stress under different water availabilities (irrigated or rainfed) in the Loess Plateau.

2. Material and methods

2.1. Study area and methodology

The Loess Plateau is located between 32°N-41°N and 101°E-114°E, with an area of about 648,700 km^2, accounting for 6.76% of the total land area of China. The topography of the Loess Plateau in the northwest is higher than that in the southeast, with the elevation declining from 3000 m to 500 m. The Loess Plateau is in a transition zone from a semi-humid to a semi-arid climate between the eastern and western part of China. The minimum average annual temperature is −3.1 and 15.3 °C in the northwest and southeast, respectively (Jiang et al., 2016). The precipitation is unevenly distributed spatially and temporally. In semi-humid areas of the southeastern part, precipitation exceeds 600 mm/yr; in semi-humid and drought-prone areas of the middle part, the precipitation is about 400–600 mm/yr; while in the semi-arid areas in the northwest, the precipitation is only 150–250 mm/yr. Temporally, the high interannual variability makes the Loess Plateau one of drought-prone areas in China. The precipitation in wet years can be two to five times than that in dry years. The Loess Plateau mainly contains mountains and hilly areas. Wheat and maize are the staple crops and are mostly rainfed. Agriculture in the Loess Plateau is characterized by smallholder farms and is mainly limited by water availability.

For this study, 158 counties in the Loess Plateau that planted winter wheat were selected according to the county statistics (Fig. 1). The sowing dates varied from September 18 to October 21, 2010, and the maturity dates varied from May 28 to July 18, 2011 for winter wheat. Twenty-one agrometeorological stations observe the growth of winter wheat in the Loess Plateau. The average precipitation at these stations was between 188.2 and 301.1 mm during the winter wheat growing seasons from 2005 to 2016, with the least precipitation occurring during the 2010–2011 growing season. In this study, we chose the winter wheat growing period from 2010 to 2011 in the Loess Platea as a case study to investigate the wheat WUE as a function of water stress under rainfed and irrigated conditions. This time period witnessed continuous droughts during the sowing and overwintering periods, which was a typical agrometeorological condition for winter wheat in the Loess Plateau.

The water requirement of winter wheat in the Loess Plateau is between 250.0 and 650.0 mm (Huang et al., 2004). During most growing seasons, precipitation was far from satisfying the water requirement of winter wheat for growth and development. In the Loess Plateau, the water sources for irrigation are mainly groundwater, reservoirs, and rivers. In most parts of the northwest Loess Plateau, irrigation may increase the winter wheat yield by 62% to 126% with respect to rainfed wheat (Liu et al., 2007).

The main content of this study includes two parts (Fig. 2): 1) the classification of irrigated and rainfed wheat, and 2) the evaluation of WUE as a function of water stress for irrigated and rainfed wheat. First, the irrigated and rainfed wheat are classified using the SVM algorithm based on the phenological parameters extracted from the MODIS NDVI time series. Next, the wheat yield is estimated using the LUE model, and WUE is estimated based on yield and ETa. Finally, the

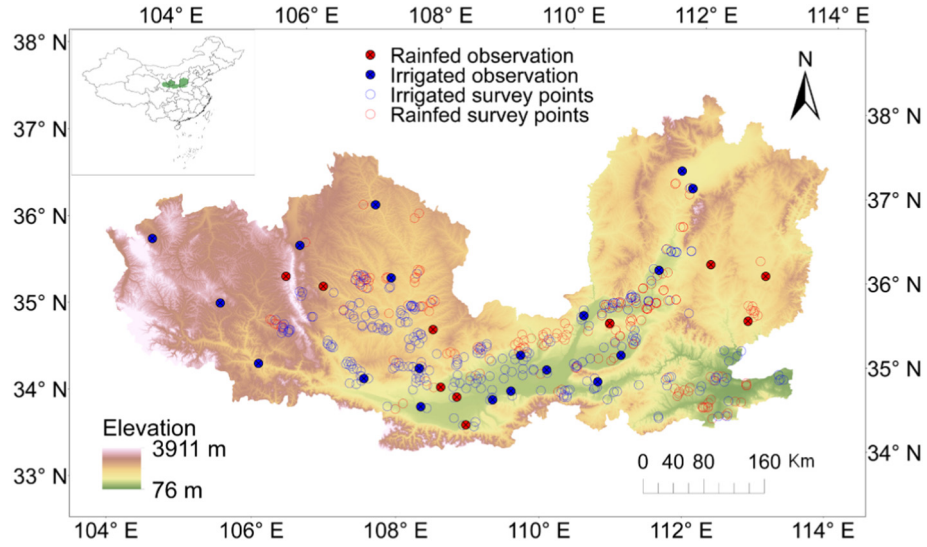

Fig. 1. Location of the Loess Plateau, digital elevation model (DEM), and field-survey sites of irrigated and rainfed wheat.

WUE of irrigated and rainfed wheat as a function of water stress is evaluated.

2.2. Data

2.2.1. Meteorological data

The study period spans from September 1, 2010 to July 31, 2011 (a total of 334 days), covering the entire growing season of winter wheat. The data from 158 meteorological stations across the Loess Plateau and Changwu station (35°12′N, 107° 40′E, 1200 m above sea level) were obtained from the China Meteorological Administration (Table S1), including daily maximum, minimum, and mean temperatures (°C), wind speed (m/s), relative humidity (%), precipitation (mm), barometric pressure (hPa), and hours of sunshine (hours). To match the spatial resolution of meteorological data with that of remote sensing data, we used a multiple linear regression equation between meteorological parameters and geographic variables (longitude, latitude, elevation, slope, and aspect) (Table S1), and the residuals were also interpolated (Ito et al., 2002). The two interpolation results were then superimposed to obtain daily raster meteorological data at a resolution of 250 m × 250 m.

2.2.2. Soil properties

The dataset of soil properties used in this study is maintained by Beijing Normal University (Dai et al., 2013) (Table S1). The dataset includes soil hydrological parameters such as the parameters of the Clapp and Hornberger functions and the van Genuchten and Mualem functions, field capacity, wilting coefficient, etc. The spatial resolution is 30 arc sec and the soil is divided into seven vertical layers with a maximum thickness of 1.38 m.

2.2.3. Agricultural meteorological observations, field survey, and county-level statistics

The data from the 21 agricultural meteorological observation stations include latitude, longitude, sowing and maturity dates, yield, and field management of winter wheat (Table S1). The ETa of winter wheat during the 2006–2007 growing season was recorded by using a large-scale weighing lysimeter at Changwu station (Table S1). The field-survey data include latitude, longitude, and irrigated or rainfed information from 481 winter wheat survey sites in the Loess Plateau. The county-level statistical data of winter-wheat yield in the Loess Plateau were obtained from the China Statistical Yearbook and Provincial Agricultural Statistical Yearbook, including planted areas, yield per unit, total yield production, etc. (Table S1).

2.2.4. Satellite remote sensing data

This study uses the MODIS NDVI data at 16-day time interval and 250 m spatial resolution, which spans the entire growing season of winter wheat from September 2010 to July 2011 (Tables S1, 2). The mosaic and projection transform were applied to the downloaded NDVI data, and then subset based on the shapefile of the Loess Plateau. Finally, the NDVI time series data that reflected the growing season characteristics of winter wheat were obtained by sequentially overlying the images.

2.3. Methods

2.3.1. Classification of irrigated and rainfed wheat

The planted areas of winter wheat and the classification of irrigated and rainfed wheat in the Loess Plateau were extracted following the method of Jin et al. (2016). Upon comparing with other landcovers, two obvious differences appear in the NDVI time series of winter wheat. The first is the increasing trend in the NDVI time series before the overwintering period, and the second is the decreasing trend in NDVI time series from tasseling to maturity. In the NDVI time series, winter wheat can be distinguished from other landcovers based on these two characteristics. The phenological parameters (sowing dates, maturity dates, etc.) were estimated, and the $NDVI_{max}$ and time-integrated NDVI were selected as characteristic variables to establish a classification model based on the SVM algorithm. The classification model was then applied to the Loess Plateau to classify irrigated and rainfed wheat. The sowing date was estimated by following the method of Lobell et al. (2013), in which the green-up date (the earliest time that crop growth can be reliably detected from satellite data) is extracted from remote sensing data. The green-up date is then offset by a fixed number of days from the sowing date. More details about the pretreatment of remote sensing data, estimating phenological parameters (e.g., sowing and maturity dates), selecting characteristic variables, and determining SVM parameters (γ and C) can be found in Jin et al. (2016).

2.3.2. Definition of water use efficiency

In this study, WUE is defined as

$$\mathrm{WUE} = \mathrm{Yield}/\mathrm{ETa} \quad (1)$$

where the unit of WUE is kg/m^3, "Yield" and "ETa" represent crop yield (kg/ha) and the actual evapotranspiration during the crop growing season (m^3/ha), respectively.

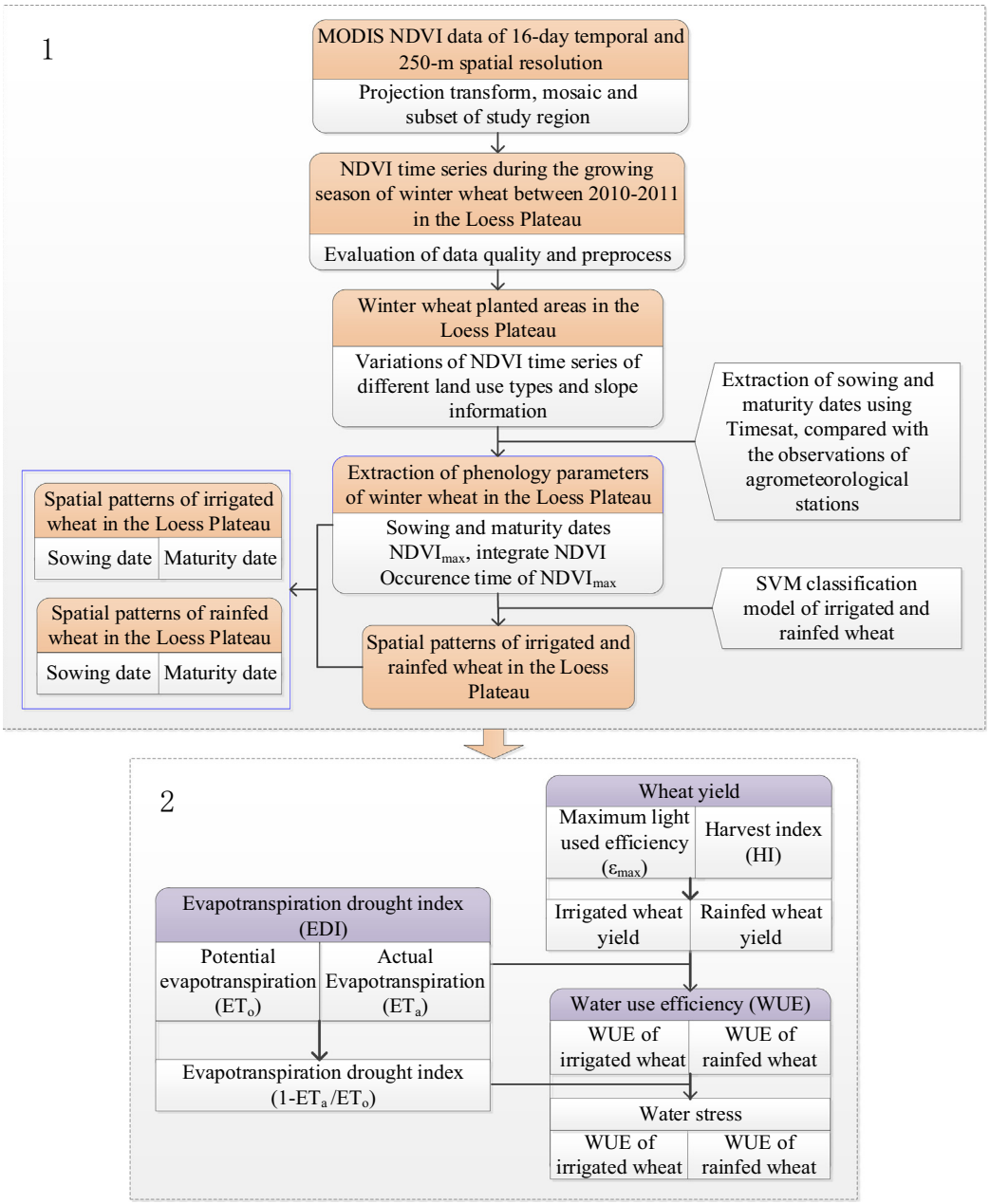

Fig. 2. Flowchart of procedure used in this study.

2.3.3. Estimation of winter wheat evapotranspiration

The crop ETa is determined by multiple factors, such as surface net radiation (Rn), temperature, NDVI, LAI, and soil moisture. In this study, the latent heat flux was estimated by using the improved Priestley–Taylor method (Yao et al., 2013). The Priestley-Taylor equation is a simplification of the Penman equation, which avoids the computation of aerodynamic and surface resistance and therefore has good operability. It requires only four input variables, i.e., Rn, NDVI, air temperature, and the range of diurnal air temperature. The total latent heat flux is the sum of soil evaporation, crop transpiration, evaporation of wet soil surface, and the evaporation of crop interception. More details of the algorithm can be found in Yao et al. (2013). The parameter α was set to 1.74 following Döll and Siebert (2002).

2.3.4. Estimation of winter wheat yield using a light use efficiency model

The LUE model has been widely used to monitor crop growth processes, and estimate crop NPP and yield (Fig. 3) (Lobell et al., 2003; Gitelson and Gamon, 2015). In this study, the formula for estimating crop yield is

$$\text{Yield} = \sum(PAR \times fPAR)\Delta t \times \varepsilon \times HI \quad (2)$$

where *PAR* is the incident photosynthetically active radiation (MJ/m^2 400–700 nm), *fPAR* is the fraction of absorbed *PAR*, ε is the LUE of the crop (g·C/MJ), Δt is the time scale (daily), and *HI* is the harvest index.

(1) Estimation of *fPAR*

The equation to estimate *PAR* is $PAR = R_s \times 0.5$, in which R_s is the solar radiation (MJ/m^2·day) and is calculated by using $R_s = (a_s + b_s \frac{n}{N}) R_a$ (Allen et al., 1998). The parameters are $a_s = 0.1776$ and $b_s = 0.5470$ (Liu et al., 2009).

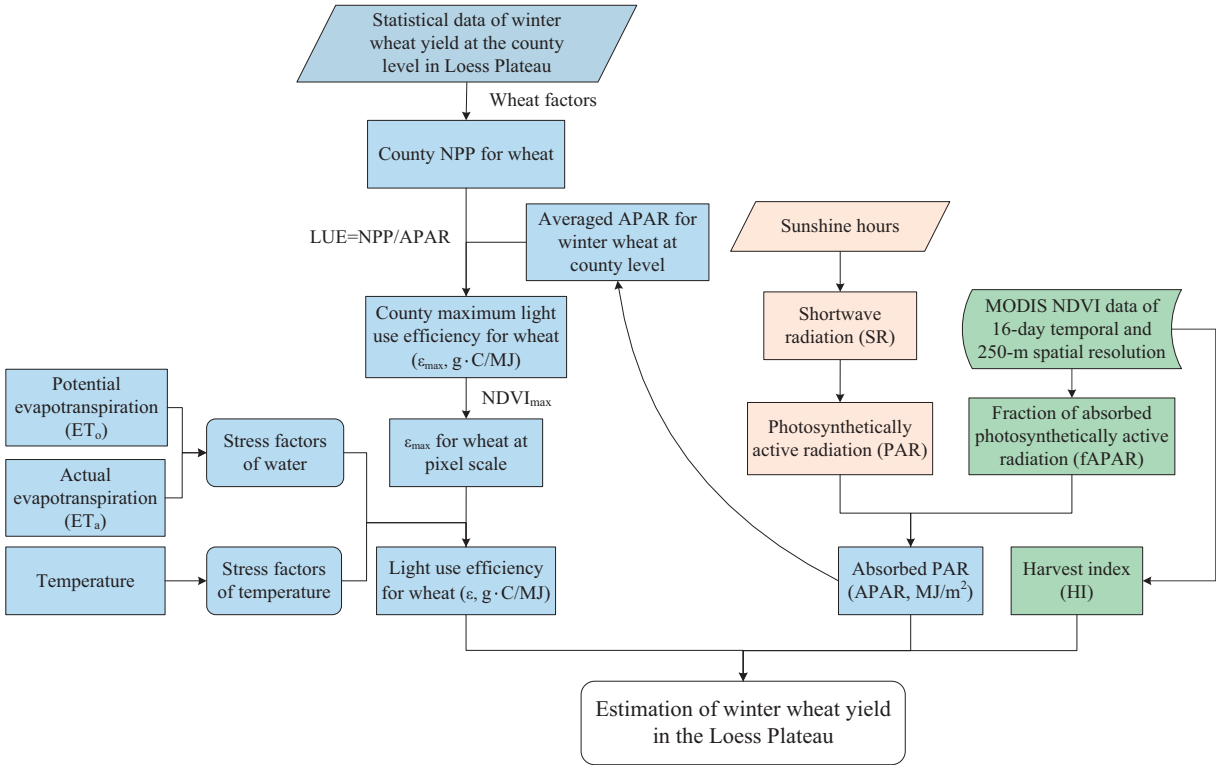

Fig. 3. Flowchart of process for estimating winter wheat yield using light use efficiency model.

The *fPAR* is calculated as the average of $fPAR_{NDVI}$ and $fPAR_{SR}$ (Lobell et al., 2003), which are estimated as follows:

$$fPAR_{NDVI} = \frac{NDVI - NDVI_{min}}{NDVI_{max} - NDVI_{min}} \times (fPAR_{max} - fPAR_{min}) + fPAR_{min} \quad (3)$$

$$fPAR_{SR} = \frac{SR - SR_{min}}{SR_{max} - SR_{min}} \times (fPAR_{max} - fPAR_{min}) + fPAR_{min} \quad (4)$$

$$SR = \frac{1 + NDVI}{1 - NDVI} \quad (5)$$

where $NDVI_{max}$ ($NDVI_{min}$) is the maximum (minimum) *NDVI* (Tao et al., 2005). SR_{max} (SR_{min}) is the 2nd (98th) percentile of *SR* over the entire study region. The values of $fPAR_{min}$ and $fPAR_{max}$ are independent of vegetation types and are set to 0.001 and 0.95, respectively (Lobell et al., 2003).

(2) Light use efficiency of winter wheat

Light use efficiency (ε) reflects the extent of photosynthetically active radiation absorbed by the crop and converted to organic carbon (g·C/MJ). It is affected by temperature and moisture conditions and can be defined as

$$\varepsilon = \varepsilon_{max} \times f(T) \times f(W) \quad (6)$$

where ε_{max} is the maximum LUE under ideal conditions, and $f(T)$ and $f(W)$ are stress factors for temperature and water, respectively. Based on the county wheat yield statistics, MODIS imagery, and meteorological data from the Loess Plateau, ε_{max} is estimated as follows:

$$\varepsilon_{max} = \frac{NPP}{r \times \sum fPAR \times PAR \times f(T) \times f(W)} \quad (7)$$

In this study, ε_{max} is adjusted according to the ratio between the $NDVI_{max}$ of each pixel and the average $NDVI_{max}$ for all pixels in the county to reflect the spatial heterogeneity of ε_{max} (Wang et al., 2010).

The county-level NPP is calculated as follows (Lobell et al., 2002):

$$NPP = \sum \frac{Yield_s \times (1 - M) \times C}{HI \times R} \quad (8)$$

where $Yield_s$ is the statistical yield of winter wheat, *M* is the water content in harvest parts (0.15), *C* is the carbon content in the harvest parts (0.39), *HI* is the winter wheat harvest index (the ratio of yield production to biomass), which is calculated at grid cell level based on the method in Moriondo et al. (2007), and *R* is the proportion of *NPP* allocated to the ground parts (0.90).

The temperature stress factor $f(T)$ is estimated as follows:

$$f(T) = \frac{(T - T_{min})(T - T_{max})}{(T - T_{min})(T - T_{max}) - (T - T_{opt})^2} \quad (9)$$

where T_{opt}, T_{min} and T_{max} are the optimum, lowest and highest temperatures for photosynthesis, whose corresponding values are 20, 0 and 37 °C, respectively (Xiao et al., 2004).

The water stress factor $f(W)$ varies from 0.5 (extreme drought condition) to 1 (very wet conditions) and reflects how available water affects the LUE. It is calculated as follows:

$$f(W) = 0.5 + 0.5 \times ETa/ETo \quad (10)$$

where *ETo* and *ETa* are the potential and actual evapotranspiration (mm), respectively.

(3) Estimation of *HI*

HI is a crop-specific parameter and is relatively stable in a given study area unless the crop suffers severe temperature or water deficit

stress. The use of *HI* at the pixel scale will be helpful to improve the accuracy of crop yield prediction. Generally, *HI* is represented as the ratio of aboveground biomass to grain yield (i.e., the proportion of carbon from the sources to the grain). Because the NDVI of crops during the critical growing period is closely related to crop biomass and yield, the NDVI time series closely reflects the growth and development of the crop. Here, we use the NDVI and the method in Moriondo et al. (2007) to estimate regional crop *HI* as follows:

$$HI = HI_{max} - HI_{range} \cdot \left(1 - \frac{NDVI_{Post}}{NDVI_{Pre}}\right) \quad (11)$$

where HI_{max} is the maximum *HI* (in this study it was 0.584) (Ji et al., 2010), HI_{range} is the possible range of *HI* (0.369), $NDVI_{Pre}$ is the mean NDVI of winter wheat from emergence to flowering, $NDVI_{Post}$ is the mean NDVI of winter wheat from anthesis to maturity. Usually, $NDVI_{Post}/NDVI_{Pre}$ are between 0 and 1, and the estimated *HI* is between the minimum and maximum ranges of *HI* (0.215 and 0.584 in this study).

2.3.5. Estimation of evapotranspiration drought index

Under drought conditions, the ETa rate is less than the ETo rate due to soil moisture restriction. Thus, the ratio of ETa to ETo reflects the drought conditions and has been widely used for drought monitoring (Su et al., 2003; Yao et al., 2010). The evapotranspiration drought index (*EDI*) is expressed as follows:

$$EDI = 1 - \frac{ETa}{ETo} \quad (12)$$

where, *ETa* and *ETo* are the cumulative actual and potential evapotranspiration during the growing season of winter wheat, respectively. Theoretically, the *EDI* values are between 0 and 1. When soil moisture is seriously reduced, the crop water-stress severity tends to increase. The gap between potential and actual evapotranspiration then increases, resulting in a larger *EDI*. The *EDI* is small when the soil moisture content is high.

3. Results

3.1. Classification of irrigated and rainfed wheat in the Loess Plateau

The statistical area of winter wheat planted in 2010–2011 in the Loess Plateau was 2.51 Mha. The planted area was 2.38 Mha, as extracted by using NDVI time series data, and the accuracy reached 95.3%. The area was then used as a basis for the subsequent classification of irrigated and rainfed wheat. The differences between reported and MODIS estimates range from −29 to 12 days for sowing dates, and from −25 to 18 days for maturity dates. The differences between average estimated sowing and maturity dates and observations are 5 and 6 days, respectively (Table S3 and Fig. S1). The $NDVI_{max}$ and time-integrated NDVI of 481 irrigated and rainfed wheat survey sites in the Loess Plateau were selected as characteristic variables to establish the SVM classification model. The highest accuracy of cross validation for test samples reached 96.2% when using the global optimal parameter sets of C and γ ($C = 0.0625$, $\gamma = 2.8284$) and screening via the five-fold cross-validation method (Fig. S2). The spatial patterns of irrigated and rainfed wheat are dispersed and cross-distributed. In general, the irrigated wheat is mainly distributed in flat regions, while the rainfed wheat is mostly cultivated in regions with high topographic relief. The proportion of rainfed and irrigated wheat in the Loess Plateau was 59.9% and 40.1%, respectively (Fig. 4).

3.2. Evapotranspiration during winter wheat growing season in the Loess Plateau

The results suggest that the ETo of winter wheat varied from 404.9 to 837.0 mm during the growing season in the Loess Plateau, with an average of 587.5 mm. The estimated ETo increased with latitude and altitude in the eastern Loess Plateau, whereas the opposite held in the western Loess Plateau. Our estimated ETa is favorably comparable with the observation data at the Changwu station ($R^2 = 0.74$, Fig. S3), which spanned the 2006–2007 winter wheat growing season (sowed on September 11, 2006 and harvested on July 26, 2007). Further analyses show that the ETa of rainfed wheat was between 207.3 and 411.9 mm, with an average of 286.9 mm. Meanwhile, the ETa of irrigated wheat was between 232.2 and 427.6 mm, with an average of 316.1 mm. This is 29.2 mm (10.2%) higher than that of rainfed wheat. When the ETa exceeded 300 mm, the frequency of the ETa of irrigated wheat significantly exceeded that of rainfed wheat. Spatially, the ETa increased from north to south for both irrigated and rainfed winter wheat (Fig. S4).

3.3. Estimate of winter wheat yield using light use efficiency model in the Loess Plateau

The wheat yield estimated by using the LUE model was validated against the 2011 wheat yield statistics at the county level. The spatial patterns were similar between the estimated and recorded yield, with $R^2 = 0.94$ (Fig. S5a and b). The spatial pattern of winter wheat yield

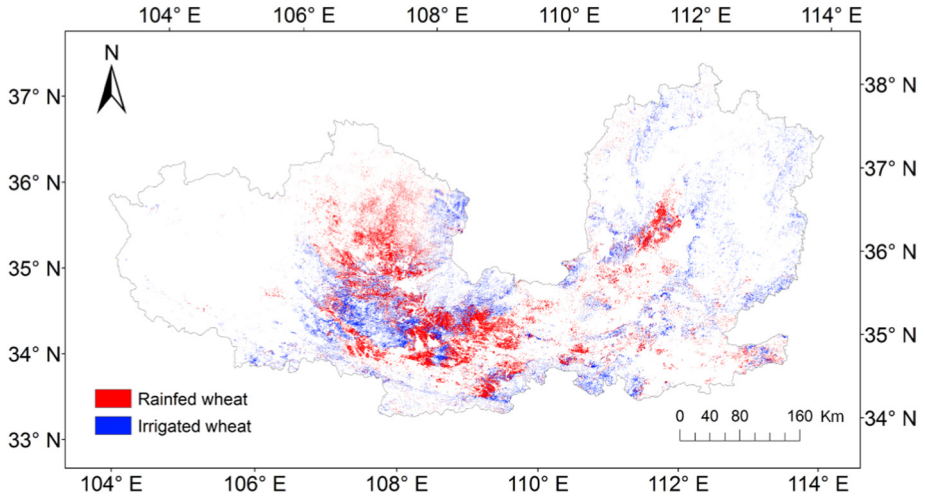

Fig. 4. Spatial patterns of irrigated and rainfed wheat in the Loess Plateau.

for the Loess Plateau is mainly determined by soil fertility and the availability of water resources. Our results suggest that, compared with rainfed wheat, the yield of irrigated wheat was higher and exhibited different significant spatial patterns. Over the rainfed wheat areas, the total precipitation during the growing season was far inferior to the growth demand of the crop. The significant spatial heterogeneity of the yield of rainfed wheat was caused by the large spatio-temporal variations in precipitation. Generally, the yield of rainfed wheat decreased from south to north in the western Loess Plateau. In the eastern part, the yield of rainfed wheat was relatively lower in the central area and higher in the peripheral areas.

These results illustrate that irrigated wheat suffered less water stress and had less spatial variations than rainfed wheat because of the additional water from irrigation. The average yield of irrigated wheat was 3928.4 kg/ha (2214.9–10,547.0 kg/ha), 22.2% higher than that of rainfed wheat (3215.7 kg/ha, ranging from 1375.3–6247.3 kg/ha) (Fig. 5a and b). The frequency of irrigated wheat was significantly greater than that of rainfed wheat when yield exceeded 3500 kg/ha (Fig. 5c). This implies that this region has the potential to further increase wheat yield if additional water were available.

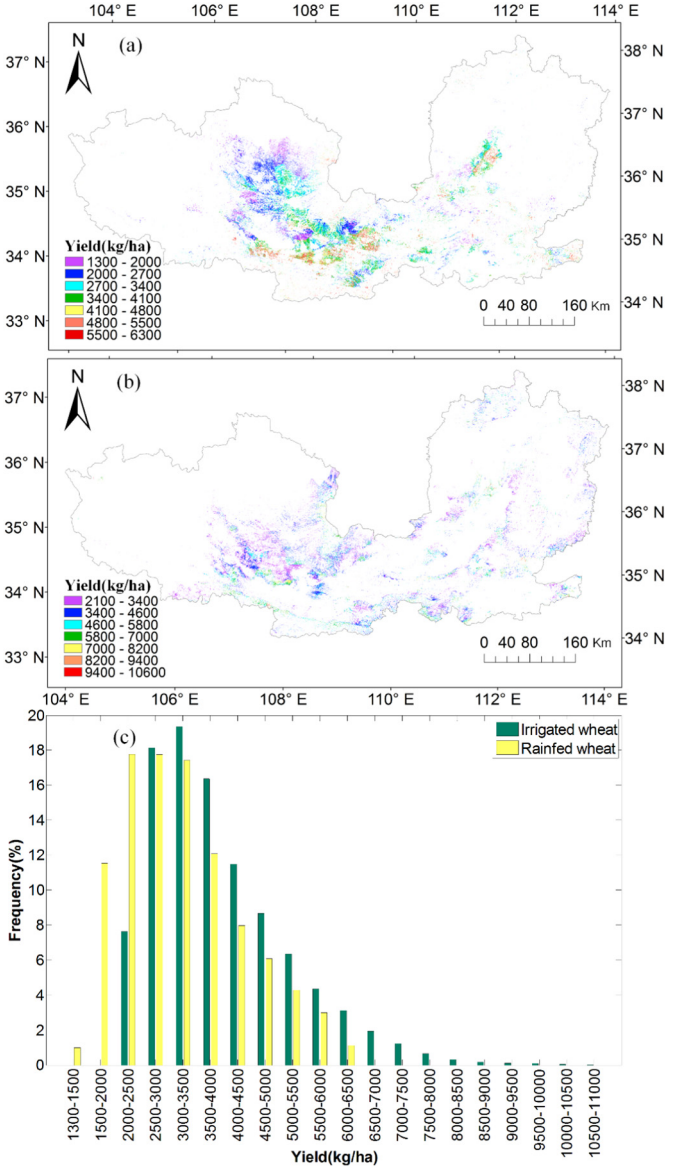

Fig. 5. Yield of (a) rainfed and (b) irrigated wheat and (c) frequency distribution for Loess Plateau.

HI and ε_{max} varied greatly at the regional scale, which may induce some mistakes and reduce the heterogeneity in the estimated yield. This is mostly because the productivity of irrigated (rainfed) wheat is underestimated (overestimated) when using the same *HI* and ε_{max} for the entire study area. The HI of winter wheat ranged from 0.26 to 0.43, with an average value of 0.31 during the study period. Spatially, it decreased from north to south in the Loess Plateau, showing uneven spatial patterns (Fig. S6). Over the study period, the spatial patterns of ε_{max} of irrigated and rainfed wheat differed significantly (Fig. S7). The mean ε_{max} of rainfed and irrigated wheat were 0.25 g·C/MJ (0.06–0.48 g·C/MJ) and 0.26 g·C/MJ (0.10–0.63 g·C/MJ), respectively.

3.4. Influence of water stress on WUE of winter wheat

The results suggest that the mean WUE of rainfed and irrigated wheat in the Loess Plateau was 1.12 kg/m^3 (0.41–2.24 kg/m^3) and 1.22 kg/m^3 (0.62–2.70 kg/m^3), respectively. The WUE of both irrigated and rainfed wheat decreased from south to north, with higher WUE for irrigated wheat. The spatial patterns of WUE were generally consistent with those of yield and evapotranspiration, i.e., high-yield was accompanied by high WUE and vice versa (Fig. 6).

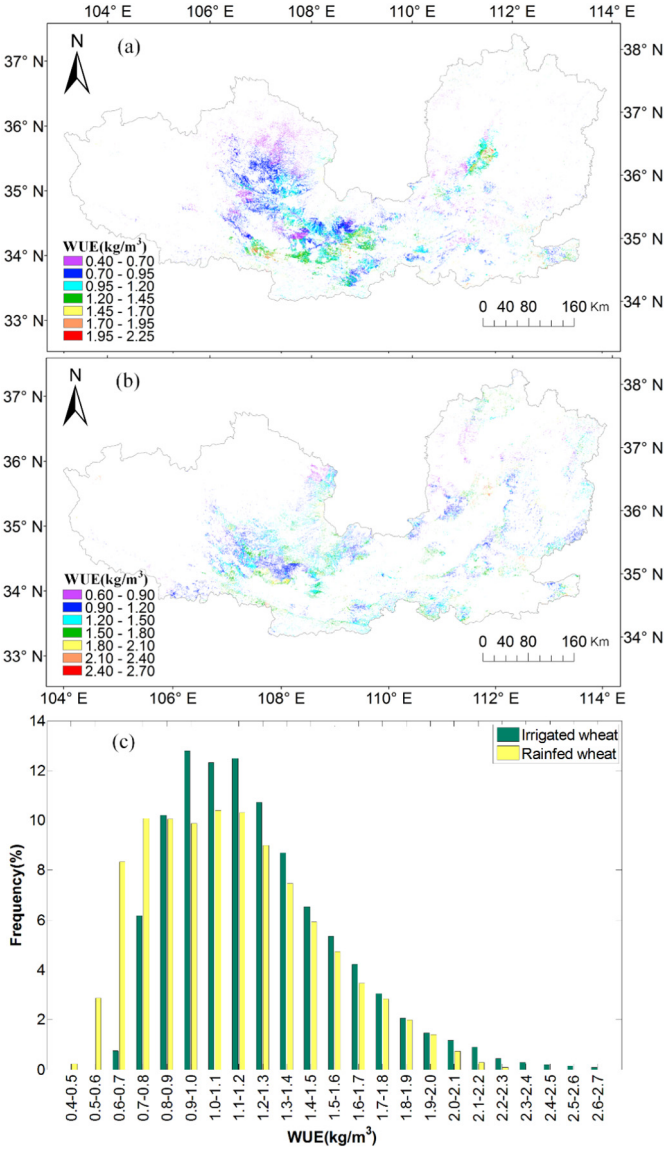

Fig. 6. WUE of (a) rainfed and (b) irrigated winter wheat and (c) frequency distribution for Loess Plateau.

The frequency distribution of irrigated wheat differed from that of rainfed wheat. When WUE was low, the WUE of irrigated wheat usually had a lower frequency than rainfed wheat, although the opposite held for irrigated and rainfed wheat upon the increasing WUE. The frequency of irrigated wheat was high when the WUE exceeded 0.8 kg/m^3. Generally, irrigated wheat had a higher WUE than rainfed wheat (Fig. 7).

In this study, the water conditions during the wheat growing season can be divided into four grades, i.e., non-water stress, mild, moderate, and severe drought. The rainfed wheat suffered more severe water stress than irrigated wheat, especially in the northern Loess Plateau (Fig. 8). During the growing season of rainfed wheat, the ratios of water stress were 17.16%, 43.32%, 21.05%, and 18.47% for non-water stress, mild, moderate, and severe drought, respectively. They were 31.55%, 45.13%, 15.23%, and 8.09% for irrigated wheat, respectively. The irrigated wheat areas without water stress were 14.39% larger than those of rainfed wheat, and the severe drought areas were 10.38% smaller than rainfed wheat. The water stress was significantly relieved by the irrigation water, and the ETa increased concomitantly. Generally, the spatial pattern of ETa was opposite that of water stress, i.e., a larger ETa correlates with less water stress.

The results show that the WUE of irrigated and rainfed wheat decreased with increasing water stress severity. The more evident decreases in rainfed wheat (Table 1) indicate that the crop WUE was strongly affected by water availability. The decrease in crop WUE under water stress may be caused by damage to electron transport and carboxylation, which reduces the capacity for carbon assimilation (Reichstein et al., 2002).

4. Discussion

4.1. Estimating winter wheat yield by using light use efficiency model

This study estimates the winter wheat yield for the Loess Plateau by using a LUE model driven by the MODIS satellite data and other multisource data. Generally, the spatial patterns of wheat yield estimated by the LUE model and statistical yield are similar, with $R^2 = 0.94$. It is noted that the winter wheat planted area of several counties in the Loess Plateau is too small to be recorded in the statistical data, where the yield of winter wheat plots identified by remote sensing data was estimated. Conversely, several counties have statistical yield data, but the winter wheat plots were too small to be identified by remote sensing data. These two aspects led to deviations in the estimated yield. The ETa during the wheat growing season was estimated by an improved Priestley–Taylor method, which only requires four input variables, such as Rn, NDVI, air temperature, and diurnal air temperature range, which are easily obtained (Yao et al., 2013). The ETa estimation method was validated by Yao et al. (2013), who used data from 16 covariance flux towers. In this study, the estimated ETa agrees well with the observed ETa ($R^2 = 0.74$).

HI and ε_{max} are two important parameters for LUE models. To accurately calculate the ecosystem productivity, ε_{max} must be realistically estimated. In many previous studies, *HI* and ε_{max} were set as constants in LUE models when estimating crop yield, such as CASA (Potter et al., 1993), VPM (Xiao et al., 2004), CFix (Veroustraete et al., 2002), and EC-LUE (Yuan et al., 2014). This would reduce the spatial heterogeneities of the estimated crop yield and introduce large uncertainties into the estimate.

In the present study, based on the county statistical wheat yield production and other ground auxiliary data, the estimated county level ε_{max} of winter wheat fell between 0.06 and 0.63 g·C/MJ during the 2010–2011 growing season in the Loess Plateau. The high yielding wheat species usually had better water supply and more field management measures at the field scale. Therefore, the ε_{max} of irrigated wheat generally exceeded than rainfed wheat. The rainfed wheat lacked an irrigation water supply and often suffered from seasonal drought, which led to a smaller ε_{max}.

The values of ε_{max} were heavily relied upon the estimation models and research scales. Chen et al. (2011) suggested that the ε_{max} of an

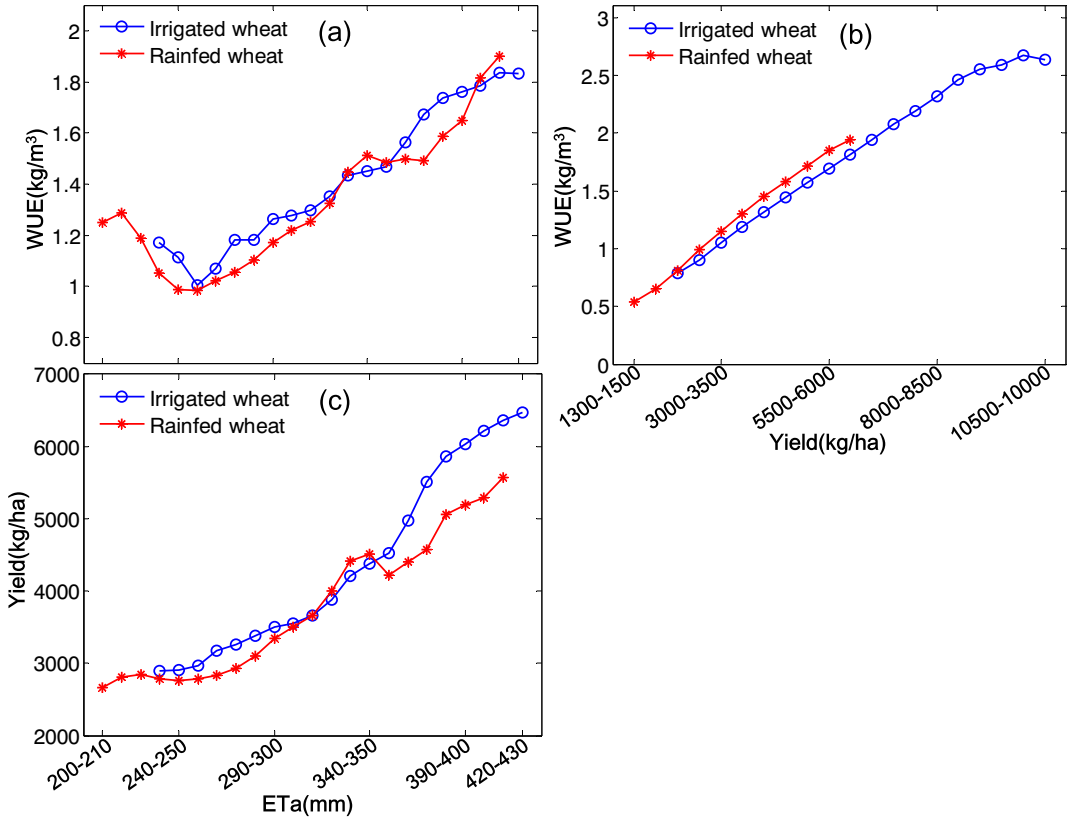

Fig. 7. Relationship between (a) ETa and WUE, (b) yield and WUE, and (c) ETa and yield for winter wheat in the Loess Plateau.

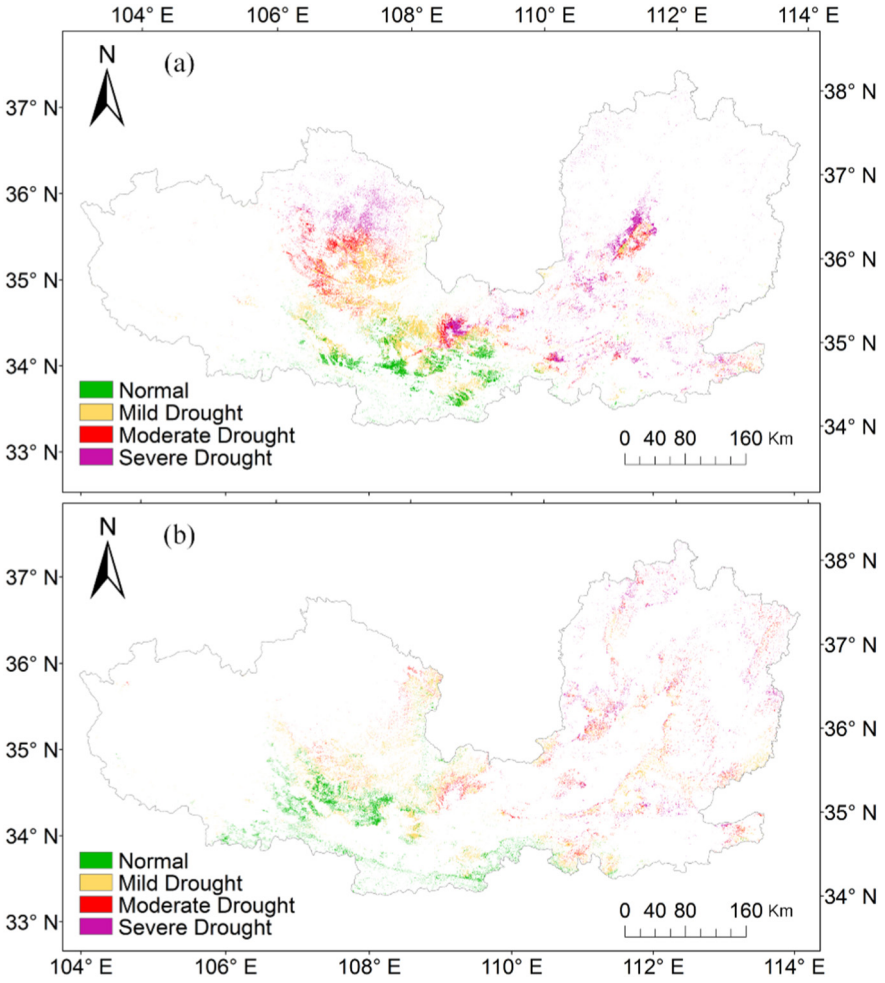

Fig. 8. Water stress during the growing season of (a) rainfed and (b) irrigated winter wheat.

agriculture ecosystem is between 0.65 and 2.00 g·C/MJ, and the value is 0.85 g·C/MJ for wheat. Wang et al. (2010) showed that the ε_{max} for farmland in northern China is between 0.76 and 0.92 g·C/MJ. Lobell et al. (2002) calculated the farmland ε_{max} based on the American county statistical yield production, and estimated a ε_{max} between 0.2 and 1.0 g·C/MJ. The ε_{max} estimated in the present study is lower than those in previous studies, which may be because of the different research scales. The values for the same state variable were not equal to each other when derived from remote sensing data with different resources and spatial resolutions. Moreover, the accuracy of the estimated ε_{max} may be reduced due to the mixed-pixel problem of multi-landcovers, such as bare soil, urban construction, other crops, etc. To better reflect the spatial heterogeneity of the estimated yield, a more reasonable parameterization scheme should be developed for the estimation of the ε_{max} in the future. The mixed-pixel problem can be solved by using remote sensing data at higher resolution and the decomposition of the mixed pixels. Generally, high spatial resolution remote sensing data are often accompanied by low temporal resolution, whereas the remote sensing data at low spatial resolution often have high temporal resolution. Thus, high spatiotemporal resolution remote sensing data can be obtained by fusioning the two types of remote sensing data, which will be of great help to improve the accuracy of the estimate of ε_{max}.

4.2. Coordinated effects of water use efficiency, evapotranspiration, and yield

Many studies have analyzed the factors influencing WUE with the goal of improving it (Liu et al., 2007; Liu et al., 2015; Rana et al., 2016). The highest WUE is not generally obtained when water supply is sufficient and crop yield is highest (Attia et al., 2016). Generally, crop yield increases linearly with increasing water consumption under deficit irrigation management, whereas WUE decreases as water supply or consumption reaches a certain degree (Trout and Dejonge, 2017). In this study, our estimated WUE falls within a reasonable range of 0.40 to 2.67 kg/m^3 (Zwart and Bastiaanssen, 2004). The variations in WUE

Table 1
Water use efficiency for winter wheat under different water conditions.

	Rainfed wheat (kg/m^3)				Irrigated wheat (kg/m^3)			
	Percent (%)	Maximum	Minimum	Mean	Percent (%)	Maximum	Minimum	Mean
No water stress	17.16	2.24	0.43	1.43	31.55	2.70	0.78	1.43
Mild drought	43.32	2.24	0.41	1.12	45.13	2.63	0.67	1.18
Moderate drought	21.05	2.24	0.44	0.98	15.23	2.02	0.62	1.07
Severe drought	18.47	2.24	0.43	0.99	8.09	1.95	0.62	0.95

depend on the synergistic effect of yield and ETa. Irrigation can increase both yield and ETa simultaneously. The present results suggest that the yield of irrigated and rainfed winter wheat increased linearly with the estimated ETa. Both the yield and ETa were higher for irrigated wheat than for rainfed wheat. When ETa increased to over 360 mm, the increased yield exceeded that of the ETa, resulting in a significantly greater WUE for irrigated wheat than for rainfed wheat. A strong linear correlation exists between WUE and yield (for irrigated wheat, WUE = $0.0002 \times \text{Yield} + 0.3185$, $R^2 = 0.988$; for rainfed wheat, WUE = $0.0003 \times \text{Yield} + 0.1596$, $R^2 = 0.996$). The WUE increased with increasing yield for both irrigated and rainfed wheat, indicating that high production capacity usually corresponds to high WUE. Thus, improving WUE is an important measure to increase crop yields.

4.3. Effects of water stress on water use efficiency

Studies at the site level and regional scales have shown that a certain soil-moisture threshold exists for WUE. Under the threshold, WUE increases with decreasing soil moisture (i.e., the vegetation ecosystem may have a high WUE under moderate water stress). Above the threshold, WUE decreases with increasing soil moisture. Lu and Zhuang (2010) found that WUE increases with increasing soil moisture under moderate drought conditions, whereas it decreases with increasing soil moisture under severe drought conditions. Some studies found that WUE tends to increase (Blum, 2009; Erice et al., 2011) whereas others found that WUE decreases under drought conditions (Reichstein et al., 2002, 2007; Dong et al., 2011). The precipitation during the growing season in the Loess Plateau is insufficient to satisfy the water demand of winter wheat growth, so the WUE of winter wheat is strongly influenced by a water deficit. The lower WUE for rainfed wheat is mainly attributed to the insufficient total water supply and high rate of soil-water evaporation. This, to a large extent, restricts the development of rainfed agriculture (Qin et al., 2013).

During the study period, the rainfed wheat suffered more severe water stress than irrigated wheat, especially in the western part of the Loess Plateau, where most of the wheat planted was rainfed. This study thus suggests that little difference between the WUE of irrigated and rainfed wheat under non-water stress conditions. The WUE of both irrigated and rainfed wheat decreased with increasing water stress. The WUE of rainfed wheat decreased more quickly, implying that the rainfed wheat was more susceptible to water stress. This result may be attributed to the limited water availability and fertility of rainfed wheat farmland. With increasing water stress, the rainfed wheat yield decreased more than the irrigated wheat yield, whereas the change in ETa was relatively small. The WUE is mainly determined by yield and evapotranspiration, and the variation of WUE depends on the sensitivity of the two components (yield and ETa) with respect to environmental changes.

4.4. Uncertainty analysis

This study estimates ε_{max} by using the statistical wheat yield at the county level in the Loess Plateau. The results of NPP were strongly influenced by the proportion it allocated to the aboveground parts (R), which had large spatiotemporal heterogeneity and was not considered in the study (Lobell et al., 2002). The errors in the statistical wheat yield may also produce some uncertainties in the estimate of NPP and yield. Furthermore, the Loess Plateau contains complex land-use types, and several land-use types may be contained in a single MODIS pixel. The estimate of ε_{max} from this study is an average value at the county level and was modified by $NDVI_{max}$. Some uncertainties in the estimated ε_{max} may be caused by mixed-pixel effects. In addition, the study does not consider uniformity conditions within the county, which may lead to an overestimate of yield for rainfed wheat and an underestimate for irrigated wheat.

5. Conclusions

In this study, we quantified the synergistic relationships between crop yield, ETa, and WUE for the winter wheat in the Loess Plateau, China. We also analyzed the wheat WUE in responds to water stress under different water management practices. The reliability of the estimated yield can be improved by considering the spatial heterogeneities of ε_{max} and *HI* when using the LUE model. Irrigation increased both yield and ETa of wheat (3928.4 kg/ha and 316.1 mm), and the induced increase in yield (22.2%) was larger than the increase in ETa (10.2%). Crop yield increased linearly with increasing ETa for irrigated and rainfed wheat, with higher increases found in irrigated wheat. Increased yield production and improved WUE can be achieved by irrigating more areas for winter wheat in the Loess Plateau.

The spatial distribution of ETa was more evident over areas where less water stress occurred. Generally, the spatial patterns of WUE were similar to the pattern of yield and ETa in the Loess Plateau, with higher WUE in the irrigated wheat. The WUE decreased with the increasing water stress for both irrigated and rainfed wheat. There was a faster decrease in WUE for rainfed wheat comparing to irrigated wheat. This result shows that the wheat WUE is greatly influenced by increasing water stress, especially for rainfed wheat. Therefore, better management practices should be applied to avoid a significant decline in WUE for rainfed wheat.

Further work is needed to extend the length of the study period to reveal the inter-annual variabilities in these variables. In addition, remote sensing data can be assimilated into crop models to better simulate crop growth and yield formation. This will be helpful to further reveal the response to water stress of crop WUE under different water management scenarios at a regional scale.

Acknowledgements

We gratefully acknowledge the support of China Postdoctoral Science Foundation (2017M613212), Special-Fund of talents (Thousand Talents Program) in Northwest A&F University (Z111021701), and National Natural Science Foundation of China (No. 41730645).

Appendix A. Supplementary data

Supplementary data to this article can be found online at https://doi.org/10.1016/j.scitotenv.2018.06.028.

References

Allen, R.G., Pereira, L.S., Raes, D., et al., 1998. Crop evapotranspiration. Guidelines for computing crop water requirements. FAO Irrigation and Drainage Paper, 56.
Attia, A., Rajan, N., Xue, Q., et al., 2016. Application of DSSAT-CERES-Wheat model to simulate winter wheat response to irrigation management in the Texas High Plains. Agric. Water Manag. 165, 50–60.
Bastiaanssen, W.G., Steduto, P., 2017. The water productivity score (WPS) at global and regional level: methodology and first results from remote sensing measurements of wheat, rice and maize. Sci. Total Environ. 575, 595–611.
Blum, A., 2009. Effective use of water (EUW) and not water-use efficiency (WUE) is the target of crop yield improvement under drought stress. Field Crop Res. 112 (2–3), 119–123.
Bu, L., Chen, X., Li, S., et al., 2015. The effect of adapting cultivars on the water use efficiency of dryland maize (*Zea mays*, L.) in northwestern China. Agric. Water Manag. 148 (148), 1–9.
Chen, T., Van, d.W., Guido, R., et al., 2011. Evaluation of cropland maximum light use efficiency using eddy flux measurements in North America and Europe. Geophys. Res. Lett. 38 (14), L14707.
Dai, Y., Shangguan, W., Duan, Q., et al., 2013. Development of a China dataset of soil hydraulic parameters using pedotransfer functions for land surface modeling. J. Hydrometeorol. 14 (3), 869–887.
Döll, P., Siebert, S., 2002. Global modeling of irrigation water requirements. Water Resour. Res. 38 (4), 8–1-8-10.
Dong, G., Guo, J., Chen, J., et al., 2011. Effects of spring drought on carbon sequestration, evapotranspiration and water use efficiency in the Songnen meadow steppe in northeast China. Ecohydrology 4 (2), 211–224.

Erice, G., Louahlia, S., Irigoyen, J.J., et al., 2011. Water use efficiency, transpiration and net CO_2 exchange of four alfalfa genotypes submitted to progressive drought and subsequent recovery. Environ. Exp. Bot. 72 (2), 123–130.
Falkenmark, M., Rockström, J., 2004. Balancing water for humans and nature: the new approach in ecohydrology. Nat. Res. Forum 2, 185.
FAO (Food and Agriculture Organization of the United Nations), 2010. AQUASTAT. Available at:. http://www.fao.org/nr/aquastat.
Gitelson, A.A., Gamon, J.A., 2015. The need for a common basis for defining light-use efficiency: implications for productivity estimation. Remote Sens. Environ. 156, 196–201.
Huang, M., Gallichand, J., Zhong, L., 2004. Water–yield relationships and optimal water management for winter wheat in the Loess Plateau of China. Irrig. Sci. 23 (2), 47–54.
Ito, M., Mitchell, M.J., Driscoll, C.T., 2002. Spatial patterns of precipitation quantity and chemistry and air temperature in the Adirondack region of New York. Atmos. Environ. 36 (6), 1051–1062.
Ji, X., Yu, Y., Zhang, W., et al., 2010. Spatial-temporal patterns of winter wheat harvest index in China in recent twenty years. China Agric. Sci. 43 (17), 3511–3519 (In Chinese).
Jiang, C., Wang, F., Zhang, H., et al., 2016. Quantifying changes in multiple ecosystem services during 2000–2012 in the Loess Plateau, China, as a result of climate variability and ecological restoration. Ecol. Eng. 97, 258–271.
Jin, N., Tao, B., Ren, W., et al., 2016. Mapping irrigated and rainfed wheat areas using multi-temporal satellite data. Remote Sens. 8 (3), 207.
Liu, J., Williams, J.R., Zehnder, A.J.B., et al., 2007. GEPIC – modelling wheat yield and crop water productivity with high resolution on a global scale. Agric. Syst. 94 (2), 478–493.
Liu, X., Mei, X., Li, Y., et al., 2009. Calibration of the Ångström-Prescott coefficients (a, b) under different time scales and their impacts in estimating global solar radiation in the Yellow River basin. Agric. For. Meteorol. 149 (3), 697–710.
Liu, Y., Xiao, J., Ju, W., et al., 2015. Water use efficiency of China's terrestrial ecosystems and responses to drought. Sci. Rep. 5 (5), 13799.
Lobell, D.B., Hicke, J.A., Asner, G.P., et al., 2002. Satellite estimates of productivity and light use efficiency in United States agriculture, 1982–98. Glob. Chang. Biol. 8 (8), 722–735.
Lobell, D.B., Asner, G.P., Ortiz-Monasterio, J.I., et al., 2003. Remote sensing of regional crop production in the Yaqui Valley, Mexico: estimates and uncertainties. Agric. Ecosyst. Environ. 94 (2), 205–220.
Lobell, D.B., Ortiz-Monasterio, J.I., Sibley, A.M., et al., 2013. Satellite detection of earlier wheat sowing in India and implications for yield trends. Agric. Syst. 115 (2), 137–143.
Lu, X.L., Zhuang, Q.L., 2010. Evaluating evapotranspiration and water-use efficiency of terrestrial ecosystems in the conterminous United States using MODIS and AmeriFlux data. Remote Sens. Environ. 114 (9), 1924–1939.
Lu, H.D., Xue, J.Q., Guo, D.W., 2016. Efficacy of planting date adjustment as a cultivation strategy to cope with drought stress and increase rainfed maize yield and water-use efficiency. Agric. Water Manag. 179, 227–235.
Mo, X., Liu, S., Lin, Z., et al., 2005. Prediction of crop yield, water consumption and water use efficiency with a SVAT-crop growth model using remotely sensed data on the North China Plain. Ecol. Model. 183 (2–3), 301–322.
Molden, D., Murrayrust, H., Sakthivadivel, R., et al., 2003. A Water-productivity Framework for Understanding and Action. pp. 1–18.
Moriondo, M., Maselli, F., Bindi, M., 2007. A simple model of regional wheat yield based on NDVI data. Eur. J. Agron. 26 (3), 266–274.
Potter, C.S., Randerson, J.T., Field, C.B., et al., 1993. Terrestrial ecosystem production: a process model based on global satellite and surface data. Glob. Biogeochem. Cycles 7 (4), 811–841.
Qin, W., Chi, B., Oenema, O., 2013. Long-term monitoring of rainfed wheat yield and soil water at the loess plateau reveals low water use efficiency. PLoS One 8 (11), e78828.
Rana, G., Ferrara, R.M., Vitale, D., et al., 2016. Carbon assimilation and water use efficiency of a perennial bioenergy crop (*Cynara cardunculus* L.) in Mediterranean environment. Agric. For. Meteorol. 217, 137–150.
Reichstein, M., Tenhunen, J.D., Roupsard, O., et al., 2002. Severe drought effects on ecosystem CO_2 and H_2O fluxes at three Mediterranean evergreen sites: revision of current hypotheses? Glob. Chang. Biol. 8 (10), 999–1017.
Reichstein, M., Ciais, P., Papale, D., et al., 2007. Reduction of ecosystem productivity and respiration during the European summer 2003 climate anomaly: a joint flux tower, remote sensing and modelling analysis. Glob. Chang. Biol. 13 (3), 634–651.
Shen, Y., Li, S., Chen, Y., et al., 2013. Estimation of regional irrigation water requirement and water supply risk in the arid region of northwestern China 1989–2010. Agric. Water Manag. 128 (10), 55–64.
Su, Z., Yacob, A., Wen, J., et al., 2003. Assessing relative soil moisture with remote sensing data: theory, experimental validation, and application to drought monitoring over the North China Plain. Phys. Chem. Earth 28 (1), 89–101.
Suyker, A.E., Verma, S.B., 2010. Coupling of carbon dioxide and water vapor exchanges of irrigated and rainfed maize-soybean cropping systems and water productivity. Agric. For. Meteorol. 150 (4), 553–563.
Tang, X., Li, H., Desai, A.R., et al., 2014. How is water-use efficiency of terrestrial ecosystems distributed and changing on Earth? Sci. Rep. 4 (4), 7483.
Tao, F., Yokozawa, M., Zhang, Z., et al., 2005. Remote sensing of crop production in China by production efficiency models: models comparisons, estimates and uncertainties. Ecol. Model. 183 (4), 385–396.
Tian, H., Lu, C., Chen, G., et al., 2011. Climate and land use controls over terrestrial water use efficiency in monsoon Asia. Ecohydrology 4 (2), 322–340.
Trout, T.J., Dejonge, K.C., 2017. Water productivity of maize in the US high plains. Irrig. Sci. 35 (3), 251–266.
Usman, M., Liedl, R., Shahid, M.A., 2014. Managing irrigation water by yield and water productivity assessment of a rice-wheat system using remote sensing. J. Irrig. Drain. Eng. 140 (7), 43–48.
Veroustraete, F., Sabbe, H., Eerens, H., 2002. Estimation of carbon mass fluxes over Europe using the C-Fix model and Euroflux data. Remote Sens. Environ. 83 (3), 376–399.
Wang, H., Jia, G., Fu, C., et al., 2010. Deriving maximal light use efficiency from coordinated flux measurements and satellite data for regional gross primary production modeling. Remote Sens. Environ. 114 (10), 2248–2258.
Wang, L., Palta, J.A., Chen, W., et al., 2018. Nitrogen fertilization improved water-use efficiency of winter wheat through increasing water use during vegetative rather than grain filling. Agric. Water Manag. 197, 41–53.
Xiao, X., Hollinger, D., Aber, J., et al., 2004. Satellite-based modeling of gross primary production in an evergreen needleleaf forest. Remote Sens. Environ. 89 (4), 519–534.
Xie, J., Chen, J., Sun, G., et al., 2016. Ten-year variability in ecosystem water use efficiency in an oak-dominated temperate forest under a warming climate. Agric. For. Meteorol. 218-219, 209–217.
Yao, Y., Liang, S., Qin, Q., et al., 2010. Monitoring drought over the conterminous United States using MODIS and NCEP Reanalysis-2 data. J. Appl. Meteorol. Climatol. 49 (8), 1665–1680.
Yao, Y., Liang, S., Cheng, J., et al., 2013. MODIS-driven estimation of terrestrial latent heat flux in China based on a modified Priestley–Taylor algorithm. Agric. For. Meteorol. 171-172 (3), 187–202.
Yuan, W., Cai, W., Xia, J., et al., 2014. Global comparison of light use efficiency models for simulating terrestrial vegetation gross primary production based on the LaThuile database. Agric. For. Meteorol. 192-193 (4), 108–120.
Zhang, Y., Kendy, E., Yu, Q., et al., 2004. Effect of soil water deficit on evapotranspiration, crop yield, and water use efficiency in the North China Plain. Agric. Water Manag. 64 (2), 107–122.
Zhang, T., Peng, J., Liang, W., et al., 2016. Spatial-temporal patterns of water use efficiency and climate controls in china's loess plateau during 2000–2010. Sci. Total Environ. 565, 105–122.
Zhang, F., Zhang, W., Qi, J., et al., 2017. A regional evaluation of plastic film mulching for improving crop yields on the Loess Plateau of China. Agric. For. Meteorol. 248, 458–468.
Zwart, S.J., Bastiaanssen, W.G.M., 2004. Review of measured crop water productivity values for irrigated wheat, rice, cotton and maize. Agric. Water Manag. 69 (2), 115–133.
Zwart, S.J., Leclert, L.M.C., 2010. A remote sensing-based irrigation performance assessment: a case study of the Office du Niger in Mali. Irrig. Sci. 28 (5), 371–385.